EPJ Web of Conferences **119**, 22004 (2016) DOI: 10.1051/epjconf/201611922004
ILRC 27

DAILY EVOLUTION OF THE INSECT BIOMASS SPECTRUM IN AN AGRICULTURAL LANDSCAPE ACCESSED WITH LIDAR

Mikkel Brydegaard [1,2,4]*, Alem Gebru[1,2,3], Carsten Kirkeby[5], Susanne Åkesson[2], Henrik Smith[2]

[1]*Lund Laser Centre (LLC), Lund University, Sölvegatan 14, 22362 Lund, Sweden, * mikkel.brydegaard@fysik.lth.se*
[2]*Centre for Animal Movement Research (CAnMove), Lund University, Sölvegatan 37, 22362 Lund, Sweden*
[3]*Laser Research Institute (LRI), Stellenbosch University, Private Bag X1, 7602 Matieland, South Africa*
[4]*Norsk Elektro Optikk AS (NEO), Prost Stabels vei 22, N-2019 Skedsmokorset, Norway*
[5]*National Veterinary Institute, Technical University of Denmark, Bülowsvej 27, 1870 Frederiksberg C, Denmark.*

ABSTRACT

We present measurements of atmospheric insect fauna intercepted by a static lidar transect over arable and pastoral land over one day. We observe nearly a quarter million of events which are calibrated to optical cross section. Biomass spectra are derived from the size distribution and presented against space and time. We discuss detection limits and instrument biasing, and we relate the insect observations to relevant ecological landscape features and land use. Future directions and improvements of the technique are also outlined.

1. BACKGROUND AND MOTIVATION

Anthropogenic exploitation of the environment, such as agricultural intensification including pesticide use, has profound effects on the atmospheric fauna in the agricultural landscape[1]. The land use may have severe negative effects on insect and natural insect predators[2,3]. The consequences of anthropogenic agricultural activity and its impact on the composition of the air-born fauna is however less known. It is expected that even specific perturbations to the population of a particular size of an organism, e.g. by using a targeted pesticide, may propagate as waves throughout the biomass spectrum, affecting populations of both smaller and larger sized organisms[4], for example through competition and the trophic chain. The effect is analogous to hole-burning spectroscopy, well known in the laser and electron population community[5].

A more heterogeneous landscape including, field borders, vegetated islands, trees, pastures used for grazing and higher variation in crop diversity is likely to have a larger abundance and diversity of the farmland insect fauna[6]. There is furthermore a current global concern about the declining pollinator fauna in the agricultural landscape[7]. Here we explore the potential of using a remote sensing technique to investigate both the diversity of the insect fauna, but also the insect occurrence in relation to field use and landscape borders. In particular, we compare the faunistic diversity between an oat field and a cattle grazed pasture at Brunslöv in south Sweden. We present the biomass spectra derived from the optical cross section (OCS) of lidar-sensed atmospheric insect fauna during one day. We define backscatter OCS as the product of diffuse reflectance and projected area, and extinction OCS as the product of ballistic opaqueness and the projected area.

2. SCENARIO AND INSTRUMENTATION

We recently developed several atmospheric CW lidars based on the Scheimpflug principle for various applications[8,9]. The lidar, shown in Fig.1, is based on telescopes on a rectangular Al crossbar - mounted on an equatorial mount with 50 kg payload capacity. The baseline separation between transmitter and receiver is 81 cm.

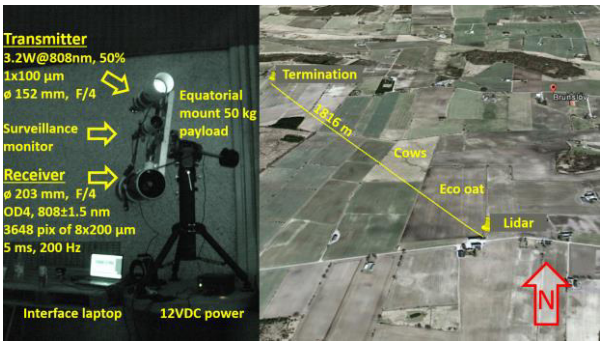

Fig.1a. *NIR photograph of the setup during field campaign.* ***1b****. The monitored transect in the vicinity of Brunslöv, southern Sweden.*

The lidar monitored a static transect of 1816 m over agricultural- and grasslands in southern Sweden. The range of interest was 30-1000 m. The lidar was positioned at 55°44'17.29"N, 13°37'48.91"E, 120 m ASL and terminated at 55°44'58.70"N, 13°36'35.25"E, 136 m ASL. The beam propagated 3-8 m over ground and the total air volume

© The Authors, published by EDP Sciences. This is an open access article distributed under the terms of the Creative Commons Attribution License 4.0 (http://creativecommons.org/licenses/by/4.0/).

monitored is estimated to 6.2 m^3. The measurements included one week continuous monitoring in mid-July, during which the sky was clear and the atmosphere homogeneous. Here we present data recorded 16th July, 2014 starting at midnight and lasting until 21:00h the following evening, at which time the sun light entered the telescope and the experiment was terminated. At this date the winds were calm 0-4 m/s, and temperatures ranged between 289-295 K.

The transmitter is a 3.2W GaAlAs diode laser emitting at 808 nm, operated at a 50% duty cycle and expanded to ø152 mm with an F/4 refractor telescope. The source slow axis is oriented perpendicular to the lidar baseline and imaged onto the termination with a final beam size of 97x452 mm.

The receiver consists of an ø203 mm F/4 Newtonian reflector telescope. Background light is suppressed by an RG780 absorption filter and a band pass filter centered at 808 nm-with a FWHM of 3 nm. The backscattered light is imaged onto a linear Si-CCD array with 3648 pixels and a pixel size of 8x200 µm. The detector is tilted 45° according to the Scheimpflug principle to obtain infinite focal depth. The detector is operated with 5 ms exposure time at 200 Hz line rate. The data are transferred via USB2, and a strobe signal is used to alternate between the dark and bright state of the laser. After interpolating and subtracting background the effective sample rate becomes 100 Hz.

3. CALIBRATION AND SENSITIVITY

The lidar generates range-time maps in files covering 10 s each. Within this time window we made three statistical measures of the 1000 lidar curves; the min-, median- and max-curve, see Fig.2. The median gives the best approximation of the static expectation value. The discrepancy between the min- and static curve, represents system noise. The range dependent threshold is defined by any events exceeding the static signal plus twice the noise (SNR=2), these were considered as atmospheric fauna. On July 16, 2014 we identified 221.684 events, or ~1.700 events / (m^3 hour).

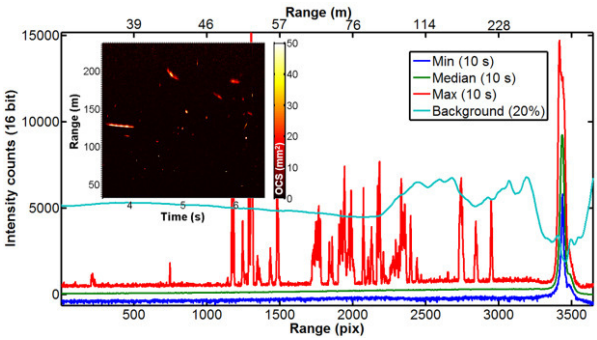

Fig.2 *Min/Median/Max/Background intensity vs. range at noon. Min indicates noise level, median static molecular air return and max atmospheric fauna. The background is rescaled to fit in the graph. The insert shows a close-up of the time-range map where insects are seen as appearing sparsely in space and time.*

The probe volume is constrained by the pixel footprints for the current experiment. To estimate the impinging laser intensity on each footprint the atmosphere is assumed to be homogeneous and insect events are divided by the static signal. Homogeneity is verified by the range-time map of the whole day. This form factor is rescaled through the known OCS, σ_{term}, for the termination; see Eq.1.

$$\sigma_{event} = \frac{\sigma_{term} r_{event}^2 \left(I_{event(r)} - I_{static(r)}\right)}{r_{term}^2 I_{static(r)}} \qquad \textit{Eq.1}$$

This calibration was verified in two ways: 1) The values relate to the apparent size derived from the opening angle (spike width) by a factor square. 2) The cross section for backscatter is one tenth of the extinction which for atmospheric insect fauna is expected to be roughly opaque with a reflectance in the order of 10% at 808 nm.

Equivalently, the noise- and CCD saturation intensity is converted into OCS providing the minimal and maximal observable OCS at any given range and time. Detection limits are 1 mm^2 at short range and 100 mm^2 at 1 km. At night time we cover a span of 1:1000 at any range, while at daytime the dynamical span is partially consumed by background and reducing to 1:100. The span within the entire range was 1:10.000. The saturation does not pose a strict limit since size may be estimated despite CCD blooming in our case.

DOI: 10.1051/epjconf/201611922004

4. STATISTICS AND BIOMASS SPECTRA

The time-range density of the aerial insect observations during the day reveals a peak activity around 13:00h which is noon in true sun time; see Fig.3. Interestingly, a rapid rush-hour is observed at the shortest range around 6:00h, lasting for only 10 minutes. As expected, activity over the cattle field is generally higher at night and peaking at dawn.

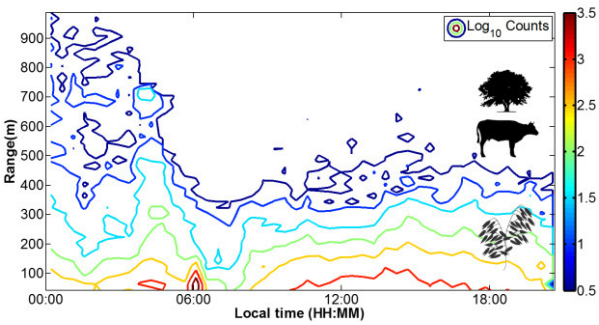

Fig.3 *Density of observations versus time and range.*

To gain further insight into the various spatio-temporal features the evolution of the biomass spectrum over the day is plotted in Fig.4. As a reference the average min and max detection limits are displayed in the background. The largest events are observed at night time, reaching sizes corresponding to birds or bats. At dawn large amounts of tiny insects are observed, and at noon the activity of intermediate sized insects peaks.

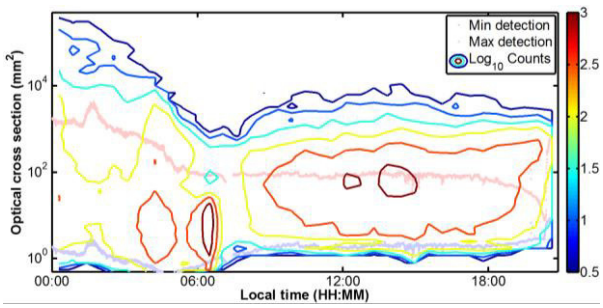

Fig.4 *Daily evolution of the biomass spectrum.*

A valid concern when comparing activity and biomass distributions at various ranges is the biasing induced by detection limits. In Fig.5 the biomass spectrum is plotted as a function of range. As a reference the average detection limits are plotted in the background. It is obvious that the biomass spectra to a large extent are associated with the observable range. However, a bimodality is observed at the shortest range, which could not be explained by instrumentation biasing. On top of this the abundance increases around 700 m range, again displaying a bimodal distribution. At this distance cattle were often resting beneath a large tree. One possible explanation for the high activity at night time and bimodal distribution over the cattle field could be blood-feeding insects or moths predated by bats. Both bats and insect are known to be attracted to solitary trees in the landscape[3].

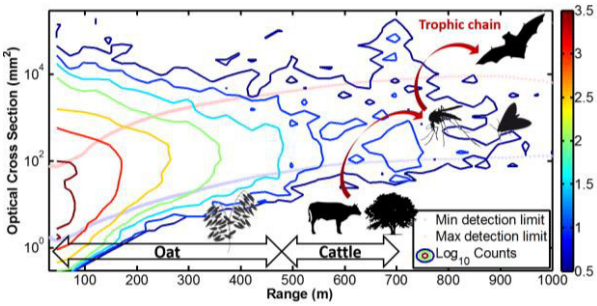

Fig.5 *The biomass spectra as a function of range is largely associated with the detection limits shown in the background. However, bimodalities are observed both in range and sizes.*

5. CONCLUSIONS AND DISCUSSION

Compared to our previous work on lidar entomology including spectral identification[10,11] and kHz modulation spectroscopy[8], the present data are crude in terms of specificity. However, it marks a record of involving a quarter million observations over a 21h period, quantities allowing for accurate distributions in several dimensions as clearly demonstrated in the figures presented in this work. Also, earlier entomological lidar work, e.g.[10,12], have not quantitatively specified cross sections and detection thresholds.

Our study shows the potential of using optical remote sensing to quantify aerial insect fauna associated with land use, farming regimes and crop type in agricultural landscapes. The method has further a great potential in identifying effects of insecticides on pollinators and pest control insects[5].

Throughout the day the temperature changes in the order of 15 K under natural field conditions, in particular when nights are clear. The lidar has weak heaters on the expander and receiver telescopes to prevent condensation in the morning, but is otherwise left drifting in temperature. This can potentially cause the laser emission wavelength to drift out of the narrow band pass filter on the receiver or the lidar structure to twist causing poor overlap of beam and FOV. Thermal stabilization, a

power monitor and adaptive overlap mechanics would improve the stability.

The projected cross section is a crude measurement of the actual organism size. Minute details in the biomass spectrum would smear out due to uncertainty regarding the phase in the wingbeat cycle, interception angle and specular reflexes from the wings. We have previously elaborated on how insect scattering can be decomposed into frequency components and assigned projection of the body (DC), wing projection (fundamental tone and low harmonics) and specular reflexes (high harmonics)[13]. In this work we also alluded to how the interception angle may be derived from the harmonics content, which may reduce the spread of cross sections for identical species.

To pursue this work we are currently upgrading the lidar with an InGaAs array detector with line rates up to 10 kHz and a SWIR laser at 1.55µm. Apart from improved sizing, additional parameters of frequency, body size and wing size, fundamental tone, harmonics spectrum[14] and wing glossiness for improved species classification can be achieved. SWIR bands also implies a 10-20 fold improvement in SNR due to the reflectance spectrum of insects[15], thus resulting in lower detection limits at longer distance.

ACKNOWLEDGEMENTS

We are grateful to the Stefan Frank for permission to work at his lands. We thank Samuel Jansson, Johan Kjellman, Tianqi Li, Sune Svanberg and Annika Södermann for assistance in field. The study was financially supported from the Swedish Research Council (621-2013-4361), an infrastructural grant from the Science Faculty at Lund University and by Lund University. This project also received funding from the Swedish Research Council through Linnaeus grants to the Centre for Animal Movement Research (349-2007-8690) and the Lund Laser Centre.

REFERENCES

[1] Grüebler, M. U., Morand, M. & Naef-Daenzer, B. 2008, A predictive model of the density of airborne insects in agricultural environments. *Agriculture, ecosystems & environment* **123**, 75-80.

[2] Wickramasinghe, L. P., Harris, S., Jones, G. & Vaughan Jennings, N. 2004, Abundance and species richness of nocturnal insects on organic and conventional farms: effects of agricultural intensification on bat foraging. *Conservation Biology* **18**, 1283-1292.

[3] Fischer, J., Stott, J. & Law, B. S. 2010, The disproportionate value of scattered trees. *Biological Conservation* **143**, 1564-1567.

[4] LawI, R., Plank, M. J., James, A. & Blanchard, J. L. 2009, Size-spectra dynamics from stochastic predation and growth of individuals. *Ecol.* **90**, 802–811.

[5] Nilsson, M., Rippe, L., Kröll, S., Klieber, R. & Suter, D. 2004, Hole-burning techniques for isolation and study of individual hyperfine transitions in inhomogeneously broadened solids demonstrated in Pr^{3+}:Y_2SiO_5. *Phys. Rev. B* **70**, 214116.

[6] Veres, A., Petit, S., Conord, C. & Lavigne, C. 2013, Does landscape composition affect pest abundance and their control by natural enemies? A review. *Agriculture, Ecosystems & Environment* **166**, 110-117.

[7] Potts, S. G. *et al.* 2010, Global pollinator declines: trends, impacts and drivers. *Trends Ecol. Evol.* **25**, 345-353.

[8] Brydegaard, M., Gebru, A. & Svanberg, S. 2014, Super resolution laser radar with blinking atmospheric particles – application to interacting flying insects *Progress In Electromagnetics Research* **147**, 141-151.

[9] Mei, L. & Brydegaard, M. 2014, Continous-wave differential absorption lidar. *Submitted.*

[10] Guan, Z. *et al.* 2010, Insect monitoring with fluorescence lidar techniques: Field experiments. *Appl. Opt.* **49**, 1-11.

[11] Runemark, A., Wellenreuther, M., Jayaweera, H., Svanberg, S. & Brydegaard, M. 2012, Rare events in remote dark field spectroscopy: an ecological case study of insects. *IEEE JSTQE* **18**, 1573 - 1582.

[12] Hoffman, D. S., Nehrir, A. R., Repasky, K. S., Shaw, J. A. & Carlsten, J. L. 2007, Range-resolved optical detection of honeybees by use of wing-beat modulation of scattered light for locating land mines. *Appl. Opt.* **46**, 3009-3012.

[13] Brydegaard, M. 2014. Towards quantitative entomological laser radar. in *ICO23. Santiago de Compostela, Spain.*

[14] Moore, A. & Miller, R. H. 2002, Automated identification of optically sensed aphid (*Homoptera: Aphidae*) wingbeat waveforms. *Ann. Entomol. Soc. Am.* **95**, 1-8.

[15] Brydegaard, M. 2014. Advantages of shortwave infrared LIDAR entomology. in *Imaging and Applied Optics 2014. Seattle, Washington.* LW2D.6 (Optical Society of America).